



Heat and mass transfer from mixed convection flow of polar fluid along a plate in porous media with chemical reaction

Heat and mass transfer

899

P.M. Patil

*Department of Mathematics, J. S. S College of Science,
Dharwad, India, and*

Ali J. Chamkha

*Manufacturing Engineering Department,
The Public Authority for Applied Education and Training,
Shuweikh, Kuwait*

Received 24 March 2011
Revised 8 October 2011
Accepted 12 December 2011

Abstract

Purpose – The purpose of this work is to study heat and mass transfer from mixed convection flow of polar fluid along a plate in porous media with chemical reaction.

Design/methodology/approach – The governing equations for this problem are solved numerically.

Findings – Polar fluids behave very differently from Newtonian fluids.

Originality/value – This work is original as little work has been reported for polar fluids.

Keywords Mixed convection, Polar fluid, Porous media, Heat generation, Chemical reaction, Forchheimer's drag, Quasi-linearization, Heat transfer, Flow

Paper type Research paper

Nomenclature

C, D	= species concentration and mass diffusivity, respectively	G	= empirical constant in the second-order resistance term
C_a, C_d	= coefficients of couple stress viscosities	Gr, Gr^*	= Grashof numbers due to temperature and concentration, respectively
C_f	= local skin-friction coefficient	I	= a constant of dimension equal to that of the moment of inertia of unit mass
C_p	= specific heat at constant pressure	k	= thermal conductivity of fluid
C_w	= surface concentration	k_1	= first-order chemical reaction rate
C_∞	= species concentration far from the surface	K	= permeability of the porous medium
Da	= Darcy number	L	= characteristic length
F	= dimensionless velocity component		
g	= acceleration due to gravity		



Authors are thankful to the anonymous Reviewers for their useful detailed comments. Dr P. M. Patil wishes to express his sincere thanks to University Grants Commission, South Western Regional Office, Bangalore, India, for the financial support under the Minor Research Project No. MRP(S)-636/09-10/KAKA060/UGC-SWRO. Also, Dr Patil dedicates this paper to one his close friends Shri B. L. Hosamani, Assistant Commissioner of Commercial Taxes, Government of Karnataka, India, who recently died in the road accident.

N	= ratio of the Grashof numbers	γ	= spin gradient velocity
Nu_x	= local Nusselt number	Γ	= Forchheimer's drag parameter
Pr	= Prandtl number	Δ	= chemical reaction parameter
q_w	= heat transfer coefficient	Θ, Φ	= dimensionless temperature and concentration, respectively
Q_0	= heat generation coefficient	ω	= angular velocity of rotation of particles
Q	= heat generation or absorption parameter	λ, λ^*	= buoyancy parameters due to temperature and concentration gradients, respectively
Re	= local Reynolds number	ξ, η	= transformed variables
Sc	= Schmidt number	ρ	= density of the fluid
Sh_x	= local Sherwood number	ε	= porosity of the porous medium
T	= temperature in the boundary layer	μ	= dynamic viscosity of the fluid
T_w	= temperature at the wall	μ_r	= rotational viscosity
T_∞	= temperature of fluid far away from the wall	ν	= kinematic viscosity
u, v	= components of velocities along and perpendicular to the plate, respectively	ν_r	= rotational kinematic viscosity
U_∞	= free stream velocity (at edge of boundary layer)	Ω	= dimensionless angular velocity
x, y	= coordinate system	<i>Subscripts</i>	
<i>Greek symbols</i>		C	= of concentration
α, β	= material parameters characterizing the polarity of the fluid	T	= of temperature
β, β^*	= volumetric coefficients of the thermal and concentration expansions, respectively	w, ∞	= conditions at the wall and infinity, respectively
		ξ, η	= denote the partial derivatives w.r.t. these variables, respectively

1. Introduction

Mixed convection flow through porous media occurs in a variety of technological and industrial applications, as well as in many natural circumstances, such as storage of nuclear waste material, packed-bed reactors, pollutant dispersion in aquifers, geothermal extraction, industrial and agricultural distribution, ground water flows, cooling of electronic components, thermal insulation engineering, food processing, casting and welding of manufacturing processes, the dispersion of chemical contaminants in various processes in the chemical industry and in the environment, soil pollution, fibrous insulation and even for obtaining approximate solutions for flow through turbo-machinery. Comprehensive theories and experiments of thermal convection in porous media and review of literature, with special emphasis on practical applications, have been reported in the recent books by Nield and Bejan (2006), Ingham and Pop (2005), Vafai (2005), Ingham *et al.* (2004) and Bejan *et al.* (2004). Merkin (1980, 1985) has studied dual solutions occurring in the problem of the mixed convection flow over a vertical surface through a porous medium with constant temperature for the case of opposing flow. Aly *et al.* (2003) and Nazar and Pop (2004) have investigated the existence of dual solutions for mixed convection in porous medium. Chin *et al.* (2007) have investigated the steady mixed convection boundary layer flow over a vertical impermeable surface embedded in a porous medium when the viscosity of the fluid varies inversely as a linear function of the temperature. In this study, both the cases of assisting and opposing flows are considered.

Problems involving combined heat and mass transfer in presence of chemical reaction are of great importance in many processes such as drying, distribution of temperature and moisture over agricultural fields and groves of fruit trees, damage of crops due to freezing, evaporation at the surface of a water body, energy transfer in a wet cooling tower and flow in a desert cooler, heat and mass transfer occur simultaneously. Chemical reactions can be modeled as either homogeneous or heterogeneous processes. This depends on whether they occur at an interface or a single phase volume reaction. A homogeneous reaction is one that occurs uniformly throughout a given phase. The species generation in a homogeneous reaction is the same as the internal source of heat generation. On the other hand, heterogeneous reaction takes place in a restricted area or within the boundary of a phase. The order of the chemical reaction depends on several factors. One of the simplest chemical reactions is the first-order reaction in which the rate of reaction is directly proportional to the species concentration. Seddeek (2005) has studied, using the finite element method, the effects of chemical reaction, variable viscosity, thermophoresis, and heat generation/absorption on a boundary layer hydromagnetic flow with heat and mass transfer over a heat surface. Kandasamy *et al.* (2005a, b) have examined the effects of chemical reaction, heat and mass transfer on with or without MHD flow with heat source/suction. Raptis and Perdiki (2006) have examined the effects of viscous flow over a non-linearly stretching sheet in the presence of chemical reaction and magnetic field.

Non-Newtonian boundary layer flows through porous medium with heat and mass transfer are seen in such wide applications as fluid film lubrication, analysis of polymer in chemical engineering, etc. The boundary layer flows for such fluids have been discussed by many research workers. Here, we shall restrict our analysis to a special family of non-Newtonian fluids, the so-called polar fluid, whose constitutive equations are characterized by Aero *et al.* (1965) and D'ep (1968), exhibits a boundary layer phenomenon. In the literature, the fluids which sustain couple stresses, called polar fluids, model those fluids with micro-structures, which are mechanically significant when the characteristic dimension of the problem is of the same order of magnitude as the size of the micro-structure. Extensive reviews of the theory can be found in the review article by Cowin (1974). Since the micro-structure size is the same as the average pore size, it is pertinent to study the flow of polar fluids through a porous medium. Examples of fluids which can be modeled as polar fluids are mud, crude oil, body fluids, lubricants with polymer additives, etc. The effects of couple stresses on the flow through a porous medium have been studied by Patil and Hiremath (1992). Hiremath and Patil (1993) have examined the effects of free convection on the oscillatory flow of a couple stress fluids through a porous medium. The effects of MHD on unsteady free convection flow past a vertical porous plate was investigated by Helmy (1998). Raptis and Takhar (1999) have discussed steady flow of a polar fluid through a porous medium by using Forchheimer's model. Kim (2001) has analyzed unsteady MHD convection flow of polar fluids past a vertical moving porous plate in a porous medium. Analytical solutions for the problem of the flow of a polar fluid past a vertical porous plate in the presence of couple stresses and radiation, where the temperature of the plate is assumed to oscillate about a mean value were reported by Ogulu (2005). Patil and Kulkarni (2008) have examined the effects of chemical reaction on free convective flow of a polar fluid through a porous medium in the presence of internal heat generation. Patil (2008) has studied the effects of free convection on the oscillatory flow of a polar fluid through a porous medium in presence of variable heat flux. Patil

and Kulkarni (2009) have examined free convective oscillatory flow of a polar fluid through a porous medium in the presence of oscillating suction and temperature.

The aim of the present study is to investigate the effects of chemical reaction and internal heat generation or absorption on the double diffusive mixed convection flow of a polar fluid through a porous medium in the presence of couple stresses. The flow configuration is modeled as hot vertical plate maintained at a constant temperature and constant species concentration bounding the porous region filled with water containing soluble and insoluble chemical materials. The system of non-linear coupled non-similar partial differential equations governing the flow is solved numerically using the method of quasi-linearization and an implicit finite difference scheme Inouye and Tate (1974) and also in a recent paper by Patil *et al.* (2010). The study reveals that the flow field is considerably influenced by the polar effects in presence of linear chemical reaction, heat source or sink and couple stresses.

2. Mathematical formulation

Consider steady, laminar, two-dimensional mixed convection flow of a viscous incompressible polar fluid through a porous medium bounded by a semi-infinite vertical porous plate embedded in a non-Darcian porous medium. The X -axis is taken along the vertical plate and the Y -axis is normal to it. The velocity, angular velocity, temperature and concentration fields are given by $(u,v,0)$, $(0,0,\omega)$, T and C , respectively. Figure 1 shows the coordinate system and physical model for the flow configuration. The surface is maintained at a constant temperature T_W and constant species concentration C_W different from the free stream temperature T_∞ and concentration

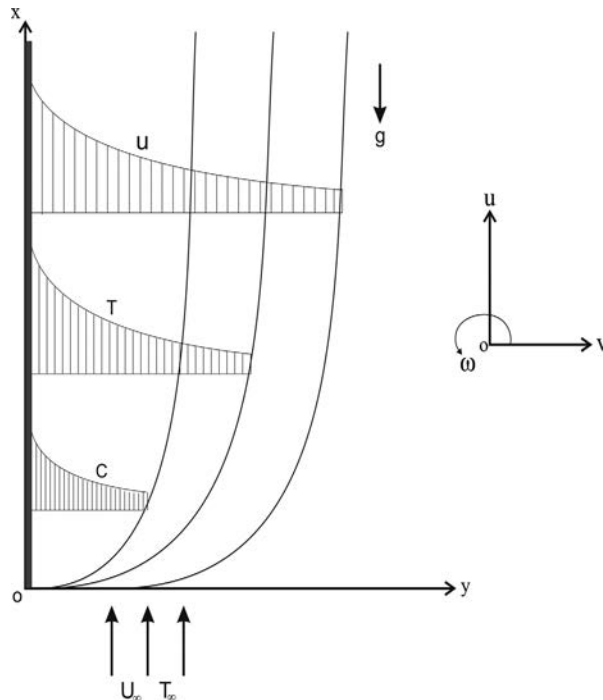


Figure 1.
The physical model and coordinate system

C_∞ sufficiently away from the surface and allows a constant suction. A heat source is placed within the flow to allow possible heat generation or absorption effects. The concentration of diffusing species is assumed to be very small in comparison with other chemical species far from the surface C_∞ and is infinitely small. Hence, the Soret and Dufour effects are neglected. A homogeneous first-order chemical reaction is assumed to take place in the flow. All thermo-physical properties of the fluid in the flow model are assumed to be constant except the density variations causing the body force term in the momentum equation. The Boussinesq approximation is invoked for the fluid properties to relate density changes to temperature and concentration changes, and to couple in this way the temperature and concentration fields to the flow field (Schlichting, 2000). Under the above assumptions, the equations of conservation of mass, momentum, angular momentum, energy and concentration governing the mixed convection boundary layer flow through porous medium are given by Aero *et al.* (1965) and Hossain *et al.* (1994):

$$\frac{\partial u}{\partial x} + \frac{\partial v}{\partial y} = 0, \quad (1)$$

$$u \frac{\partial u}{\partial x} + v \frac{\partial u}{\partial y} = (\nu + \nu_r) \frac{\partial^2 u}{\partial y^2} + 2\nu_r \frac{\partial \omega}{\partial y} + g[\beta(T - T_\infty) + g\beta^*(C - C_\infty)] - \frac{\varepsilon(\nu + \nu_r)}{K}(u - U_\infty) - \frac{G\varepsilon^2}{K^{1/2}}(u^2 - U_\infty^2), \quad (2)$$

$$u \frac{\partial \omega}{\partial x} + v \frac{\partial \omega}{\partial y} = \frac{\gamma}{I} \frac{\partial^2 \omega}{\partial y^2}, \quad (3)$$

$$u \frac{\partial T}{\partial x} + v \frac{\partial T}{\partial y} = \frac{\lambda}{\rho C_p} \frac{\partial^2 T}{\partial y^2} + \frac{Q_0}{\rho C_p}(T - T_\infty), \quad (4)$$

$$u \frac{\partial C}{\partial x} + v \frac{\partial C}{\partial y} = D \frac{\partial^2 C}{\partial y^2} - k_1(C - C_\infty) \quad (5)$$

where $\gamma = (C_a + C_d)I^{-1}$ and all parameters appearing in the subsequent and following equations are defined in the Nomenclature section.

The appropriate boundary conditions for the problem under consideration are given by:

$$\begin{aligned} y = 0 : \quad & u = 0, \quad v = 0, \quad \frac{\partial \omega}{\partial y} = -m \frac{\partial^2 u}{\partial y^2}, \quad T = T_w, \quad C = C_w, \\ y \rightarrow \infty : \quad & u \rightarrow U_\infty, \quad \omega \rightarrow 0, \quad T \rightarrow T_\infty, \quad C \rightarrow C_\infty. \end{aligned} \quad (6)$$

The boundary conditions (6) are derived from the assumption that the couple stresses are dominant during the rotation of the particles (D'ep, 1968). Further, m is a constant and $0 \leq m \leq 1$. The case $m = 0$, which corresponds to $(\partial \omega / \partial y) = 0$ at the wall represents concentrated particle flows in which the micro elements close to the wall surface are not able to rotate. This case is known as strong concentration of micro elements. The case $m = 0.5$, which corresponds to the vanishing of antisymmetric

part of the stress tensor and indicates weak concentration of micro elements. The case $m = 1.0$, which corresponds to the modeling of turbulent boundary layer flows. Here, we shall consider the case of $m = 0.5$.

Defining the stream function $\psi(x, y)$ in the usual way as:

$$u = \frac{\partial \psi}{\partial y}, \quad v = -\frac{\partial \psi}{\partial x}, \quad (7)$$

and substituting the following non-dimensional quantities:

$$\begin{aligned} \xi &= \frac{x}{L}, \quad \eta = \left(\frac{U_\infty}{\nu x}\right)^{1/2} y, \quad \psi(x, y) = (\nu U_\infty x)^{1/2} f(\xi, \eta), \\ \omega &= \left(\frac{U_\infty}{\nu x}\right)^{1/2} U_\infty \Omega(\xi, \eta), \quad u = U_\infty \frac{\partial f}{\partial \eta}, \\ v &= -\frac{(\nu U_\infty x)^{1/2}}{2x} (f(\xi, \eta) + 2\xi f_\xi - \eta f_\eta); \quad \alpha = \frac{\nu_r}{\nu}; \quad \beta = \frac{I\nu}{\gamma}; \\ \text{Re} &= \frac{U_\infty L}{\nu}; \quad \text{Da} = \frac{K}{\varepsilon L^2}; \quad (T - T_\infty) = (T_W - T_\infty) \Theta(\xi, \eta); \\ (C - C_\infty) &= (C_W - C_\infty) \Phi(\xi, \eta); \quad Q = \frac{Q_0 L}{\rho C_p U_\infty}; \quad \text{Gr} = \frac{g\beta(T_W - T_\infty)L^3}{\nu^2}; \\ \text{Gr}^* &= \frac{g\beta^*(C_W - C_\infty)L^3}{\nu^2}; \quad \lambda = \frac{\text{Gr}}{\text{Re}^2}; \quad \lambda^* = \frac{\text{Gr}^*}{\text{Re}^2}; \quad N = \frac{\lambda^*}{\lambda}; \\ \text{Pr} &= \frac{\rho\nu C_p}{k}; \quad \Delta = \frac{k_1 L}{U_\infty}; \quad \text{Sc} = \frac{\nu}{D}; \quad \Gamma = \frac{G\varepsilon^{3/2}}{K^{1/2}} \end{aligned} \quad (8)$$

into equations (2)-(5) obtains the following non-dimensional equations:

$$\begin{aligned} F_{\eta\eta} + \frac{f}{2(1+\alpha)} F_\eta - \frac{\xi}{\text{Da Re}} (F - 1) - \frac{\Gamma\xi}{(1+\alpha)} (F^2 - 1) + \frac{2\alpha}{(1+\alpha)} \Omega_\eta \\ + \frac{\lambda}{(1+\alpha)} \xi(\Theta + N\Phi) = \frac{\xi}{(1+\alpha)} [FF_\xi - f_\xi F_\eta] \end{aligned} \quad (9)$$

$$\Omega_{\eta\eta} + \beta \frac{f}{2} \Omega_\eta + \frac{\beta}{2} F\Omega = \beta\xi [F\Omega_\xi - f_\xi \Omega_\eta], \quad (10)$$

$$\Theta_{\eta\eta} + \frac{\text{Pr}f}{2} \Theta_\eta + \text{Pr} Q\xi\Theta = \text{Pr} \xi [F\Theta_\xi - f_\xi \Theta_\eta], \quad (11)$$

$$\Phi_{\eta\eta} + \frac{\text{Sc}f}{2} \Phi_\eta - \text{Sc}\Delta\xi\Phi = \text{Sc}\xi [F\Phi_\xi - f_\xi \Phi_\eta], \quad (12)$$

and the boundary conditions (6) reduce to the following non-dimensional form:

$$\begin{aligned} \eta = 0: \quad F = 0, \quad \Omega_\eta = -\frac{1}{2}F_{\eta\eta}, \quad \Theta = 1, \quad \Phi = 1, \\ \eta \rightarrow \infty: \quad F \rightarrow 1, \quad \Omega \rightarrow 0, \quad \Theta \rightarrow 0, \quad \Phi \rightarrow 0. \end{aligned} \quad (13)$$

The momentum equation (9) is coupled with all the other equations of the system. The material parameter α appearing in equation (9) is the non-dimensional parameter representing the ratio between the rotational kinematic viscosity (ν_r) and kinematic viscosity (ν). Another material parameter β appearing in equation (10) is a non-dimensional parameter representing the ratio between the kinematic viscosity and coefficients of couple stress viscosities. Both of the material parameters α and β characterize the polarity of the fluid. When $\alpha = 0$ and $\beta = 0$, the problem reduces to the corresponding Newtonian fluid case. The ratio of Grashof numbers N appearing in equation (9) is the non-dimensional parameter representing the ratio between the buoyancy force due to concentration difference and the buoyancy force due to temperature difference. N is zero for no buoyancy effect due to mass diffusion, infinite for no buoyancy effect due to thermal diffusion, and is unity for thermal and mass buoyancy forces of the same strength. It is also positive (>0) for the case in which the combined buoyancy forces are driving or assisting the flow and negative (<0) when the buoyancy forces are opposing each other. The heat generation or absorption parameter Q appearing in equation (11) is the non-dimensional parameter based on the amount of heat generated or absorbed per unit volume is $Q_0(T - T_\infty)$, Q_0 being constant coefficient, which may take either positive or negative values. The source term represents the heat generation when Q is positive (>0) and the heat absorption when Q is negative (<0). Q is zero for no heat source. The chemical reaction parameter Δ appearing in equation (12) is the non-dimensional parameter representing the generation or consumption of the diffusing species. Δ is positive (>0) for species generation, negative (<0) for species consumption and is zero for no chemical reaction.

The quantities of physical interest, namely, the skin-friction coefficient ($\text{Re}^{1/2}C_f$), wall couple stress coefficient C_{mf} , local Nusselt number ($\text{Re}^{-1/2}Nu_x$) and the local Sherwood number ($\text{Re}^{-1/2}Sh_x$) are defined, respectively, as follows:

$$\begin{aligned} C_f &= (\mu + \mu_r) \frac{\partial u / \partial y}{(1/2)\rho U_\infty^2} = 2(1 + \alpha)\text{Re}^{-1/2}\xi^{-1/2}F_\eta(\xi, 0), \quad \text{i.e. } C_f\text{Re}^{1/2} \\ &= 2(1 + \alpha)\xi^{-1/2}F_\eta(\xi, 0). \end{aligned} \quad (14)$$

$$C_{mf} = \frac{\gamma}{I\mu U_\infty} \frac{\partial \omega}{\partial y} = \left(\frac{U_\infty}{\mu L}\right) (\xi\beta)^{-1}\Omega_\eta(\xi, 0). \quad (15)$$

$$\begin{aligned} Nu_x &= -x \frac{\partial T / \partial y}{(T_w(x) - T_\infty)} = -\text{Re}^{1/2}\xi^{1/2}\Theta_\eta(\xi, 0), \quad \text{i.e. } \text{Re}^{-1/2}Nu_x \\ &= -\xi^{1/2}\Theta_\eta(\xi, 0). \end{aligned} \quad (16)$$

$$Sh_x = -x \frac{\partial C / \partial y}{(C_w(x) - C_\infty)} = -Re^{1/2} \xi^{1/2} \Phi_\eta(\xi, 0), \text{ i.e. } Re^{-1/2} Sh_x = -\xi^{1/2} \Phi_\eta(\xi, 0). \quad (17)$$

3. Method of solution

The set of non-dimensional equations (9)-(12) under the boundary conditions (13) have been solved numerically using an implicit finite difference scheme in combination with the quasi-linearization technique by Inouye and Tate (1974) and also in a recent paper by Patil *et al.* (2010). An iterative sequence of linear equations is carefully constructed to approximate the nonlinear equations (9)-(12) under the boundary conditions (13) achieving quadratic convergence and monotonicity. By applying quasi-linearization technique, the non-linear coupled ordinary differential equations (9)-(12) with the boundary conditions (13) are replaced by the following sequence of linear ordinary differential equations:

$$F_{\eta\eta}^{(i+1)} + A_1^i F_\eta^{(i+1)} + A_2^i F^{(i+1)} + A_3^i F_\xi^{(i+1)} + A_4^i \Omega_\eta^{(i+1)} + A_5^i \Theta^{(i+1)} + A_6^i \Phi^{(i+1)} = A_7^i, \quad (18)$$

$$\Omega_{\eta\eta}^{(i+1)} + B_1^i \Omega_\eta^{(i+1)} + B_2^i \Omega^{(i+1)} + B_3^i \Omega_\xi^{(i+1)} + B_4^{(i+1)} F^{(i+1)} = B_5^i, \quad (19)$$

$$\Theta_{\eta\eta}^{(i+1)} + C_1^i \Theta_\eta^{(i+1)} + C_2^i \Theta^{(i+1)} + C_3^i \Theta_\xi^{(i+1)} + C_4^i F^{(i+1)} = C_5^i, \quad (20)$$

$$\Phi_{\eta\eta}^{(i+1)} + D_1^i \Phi_\eta^{(i+1)} + D_2^i \Phi^{(i+1)} + D_3^i \Phi_\xi^{(i+1)} + D_4^i F^{(i+1)} = D_5^i, \quad (21)$$

where:

$$A_1^i = (1 + \alpha)^{-1} \left[\frac{f}{2} + \xi f_\xi \right], \quad A_2^i = -\xi \left[\frac{1}{Da Re} + \frac{F_\xi + 2\Gamma F}{(1 + \alpha)} \right], \quad A_3^i = -\frac{\xi}{1 + \alpha} F,$$

$$A_4^i = \frac{2\alpha}{1 + \alpha}, \quad A_5^i = \frac{\xi}{1 + \alpha} \lambda, \quad A_6^i = \frac{\xi}{1 + \alpha} \lambda N,$$

$$A_7^i = -\xi \left[\frac{\Gamma F^2 + FF_\xi}{(1 + \alpha)} + \frac{1}{Da Re} + \frac{\Gamma}{(1 + \alpha)} \right], \quad B_1^i = \beta \left[\frac{f}{2} + \xi f_\xi \right], \quad B_2^i = \frac{\beta}{2} F,$$

$$B_3^i = -\beta \xi F, \quad B_4^i = \beta \left[\frac{\Omega}{2} - \xi \Omega_\xi \right], \quad B_5^i = \beta \left[\frac{\Omega}{2} - \xi \Omega_\xi \right] F,$$

$$C_1^i = Pr \left[\frac{f}{2} + \xi f_\xi \right], \quad C_2^i = Pr \xi Q, \quad C_3^i = -Pr \xi F, \quad C_4^i = -Pr \xi \Theta_\xi,$$

$$C_5^i = -Pr \xi \Theta_\xi F, \quad D_1^i = Sc \left[\frac{f}{2} + \xi f_\xi \right], \quad D_2^i = -Sc \xi \Delta, \quad D_3^i = -Sc \xi F,$$

$$D_4^i = -Sc \xi \Phi_\xi, \quad D_5^i = -Sc \xi F \Phi_\xi.$$

The coefficient functions with iterative index i are known and the functions with iterative index $(i + 1)$ are to be determined. The boundary conditions are given by:

$$\begin{aligned}
 F^{(i+1)} = 0, \quad \Omega_\eta^{(i+1)} = -\frac{1}{2}F_\eta^{(i+1)}, \quad \Theta^{(i+1)} = 1, \quad \Phi^{(i+1)} = 1 \text{ at } \eta = 0, \\
 F^{(i+1)} \rightarrow 1, \quad \Omega^{(i+1)} \rightarrow 0, \quad \Theta^{(i+1)} \rightarrow 0, \quad \Phi^{(i+1)} \rightarrow 0 \text{ as } \eta \rightarrow \infty
 \end{aligned}
 \tag{22}$$

Since the method is explained by Inouye and Tate (1974) and also in a recent paper by Patil *et al.* (2010), its detailed analysis is not presented here for the sake of brevity. In brief, the non-linear coupled ordinary differential equations were replaced by an iterative sequence of linear equations following quasi-linearization technique. The resulting sequences of linear ordinary differential equations were expressed in difference form using central difference scheme in η -direction. In each iteration step, the equations were then reduced to a system of linear algebraic equations with a block tri-diagonal structure which is solved by using the Varga's algorithm (Varga, 2000).

To ensure the convergence of the numerical solution to exact solution, the step size $\Delta\eta$ and the edge of the boundary layer have been optimized and the result presented here are independent of the step size at least up to the fifth decimal place. The step size of $\Delta\eta$ has been taken as 0.001. A convergence criterion based on the relative difference between the current and previous iteration values is employed. When the difference reaches less than 10^{-5} , the solution is assumed to have converged and the iterative process is terminated.

4. Result and discussion

The numerical computations have been carried out for various values of the parameters, namely, $\alpha(0.0 \leq \alpha \leq 1.5)$, $\beta(2.0 \leq \beta \leq 10.0)$, $N(-1.0 \leq N \leq 5.0)$, $\lambda(-0.4 \leq \lambda \leq 100.0)$, $Sc(0.22 \leq Sc \leq 2.57)$, $Q(-1.0 \leq Q \leq 1.0)$, $\Delta(-0.5 \leq \Delta \leq 0.5)$, $\Gamma(0 \leq \Gamma \leq 2)$, $Pr(0.7 \leq Pr \leq 7.0)$ and $Da(1.0 \leq Da \leq 1000000.0)$. The edge of the boundary layer η_∞ is taken between 3.0 and 10.0 depending on the values of the parameters. The results have been obtained for both polar fluid and corresponding flow problem of a Newtonian (viscous) fluid.

The effects of the ratio of buoyancy forces parameter (N) and the Darcy number (Da) on the velocity $F(\xi, \eta)$, angular velocity $\Omega(\xi, \eta)$, temperature $\Theta(\xi, \eta)$ and concentration $\Phi(\xi, \eta)$ profiles are shown in Figures 2-9. The velocity $F(\xi, \eta)$ and skin-friction coefficient ($Re^{1/2}C_f$) profiles for different values buoyancy ratio parameter (N) and Darcy number (Da) are shown in Figures 2 and 3, respectively. It is observed from Figure 2 that, for positive values of the ratio of buoyancy forces aiding flow ($N > 0$), the buoyancy forces show significant overshoot in the velocity profiles near the wall. The physical reason is that the due to combined effects of assisting buoyancy forces due to thermal and concentration gradients and heat generation acts like a favorable pressure gradient which enhances the fluid acceleration. The magnitude of the overshoot decreases for negative values of the buoyancy ratio opposing flow ($N < 0$). Further, it is observed that the velocity decreases in the presence of a porous medium as compared to the case without a porous medium ($Da \rightarrow \infty$). The effects of N (the ratio of buoyancy forces) and Darcy number (Da) on the skin-friction coefficient ($Re^{1/2}C_f$) when $\lambda = 1.0$, $\beta = 2.0$, $Sc = 2.57$, $\Delta = 0.5$, $Pr = 0.7$, $Re = 10.0$, $\alpha = 0.5$, $\Gamma = 1$ and $Q = 0.5$ are shown in Figure 3. The results reveal that the skin-friction coefficient ($Re^{1/2}C_f$) increases with N for both negative and positive values monotonously. This is due to the fact that the increase of N enhances the fluid acceleration and hence,

Figure 2.
Effects of N and Da on
velocity profile for $\lambda = 2$,
 $\alpha = 1$, $\beta = 2$, $\Delta = 0.5$,
 $\xi = 0.5$, $\Gamma = 1$, $Re = 5$,
 $Sc = 0.22$, $Q = 0.5$ and
 $Pr = 0.7$

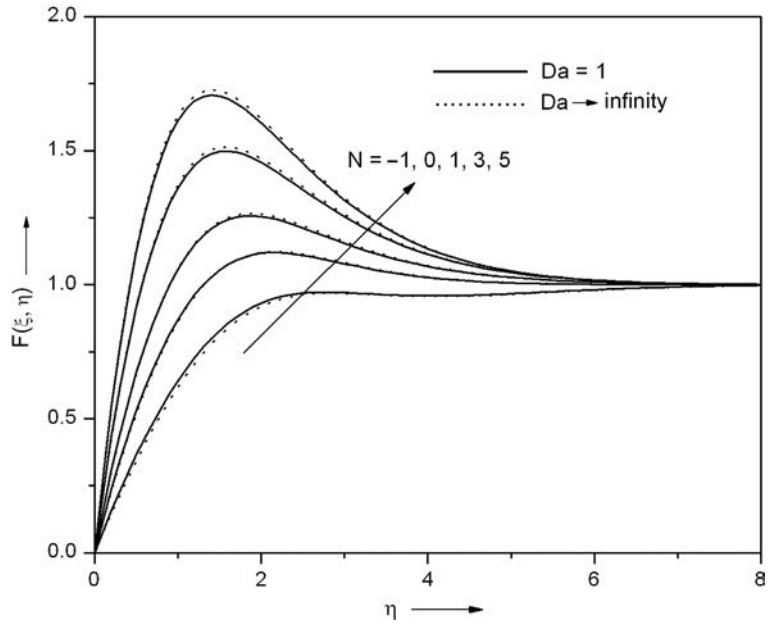
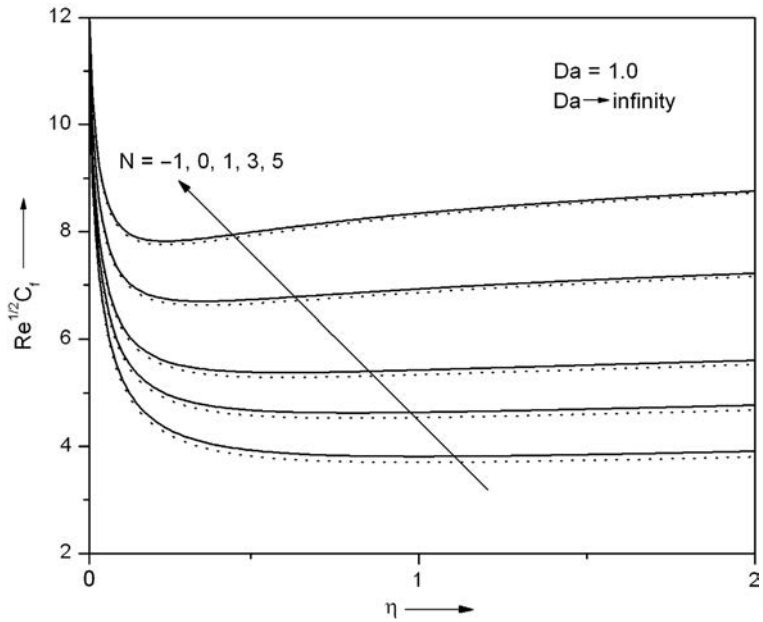


Figure 3.
Effects of N and Da on
skin-friction coefficient for
 $Re = 10$, $\alpha = 0.5$, $\beta = 2$,
 $\lambda = 1$, $\Delta = 0.5$, $Q = 0.5$,
 $Pr = 0.7$, $Sc = 2.57$ and
 $\Gamma = 1$



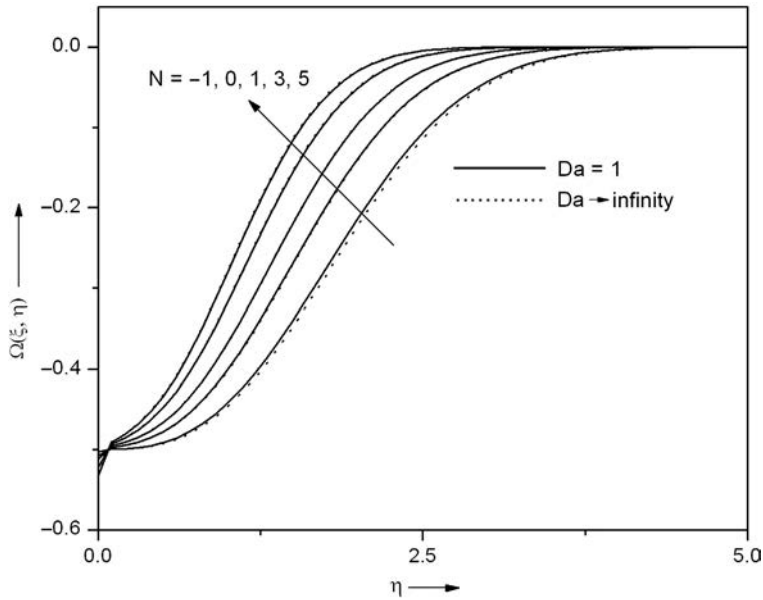


Figure 4. Effects of N and Da on angular velocity profile for $\lambda = 2, \alpha = 1, \beta = 2, \Delta = 0.5, \xi = 0.5, \Gamma = 1, Re = 5, Sc = 0.22, Q = 0.5$ and $Pr = 0.7$

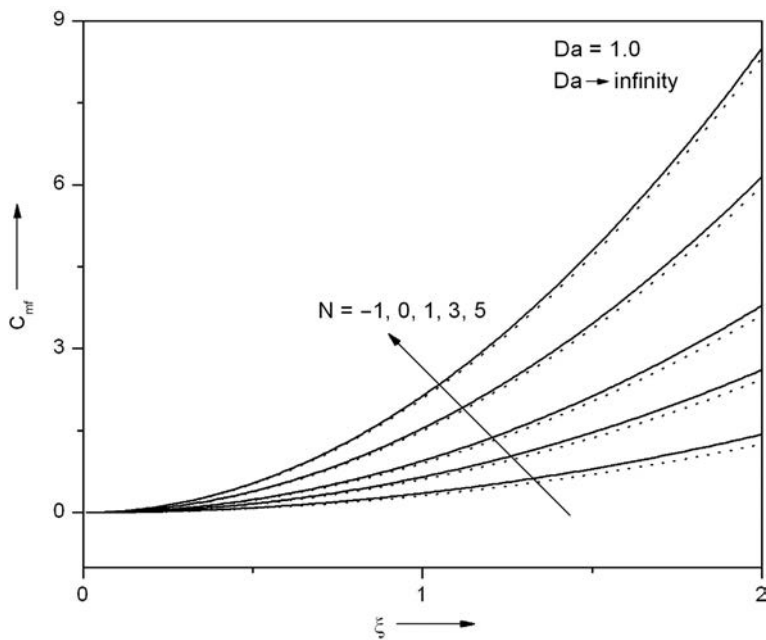


Figure 5. Effects of N and Da on couple stress coefficient for $Re = 10, \alpha = 0.5, \beta = 2, \lambda = 1, \Delta = 0.5, Q = 0.5, Pr = 0.7, Sc = 2.57$ and $\Gamma = 1$

Figure 6.
Effects of N and Da on
temperature profile for
 $\lambda = 2, \alpha = 1, \beta = 2,$
 $\Delta = 0.5, \xi = 0.5, \Gamma = 1,$
 $Re = 5, Sc = 0.22, Q = 0.5$
and $Pr = 0.7$

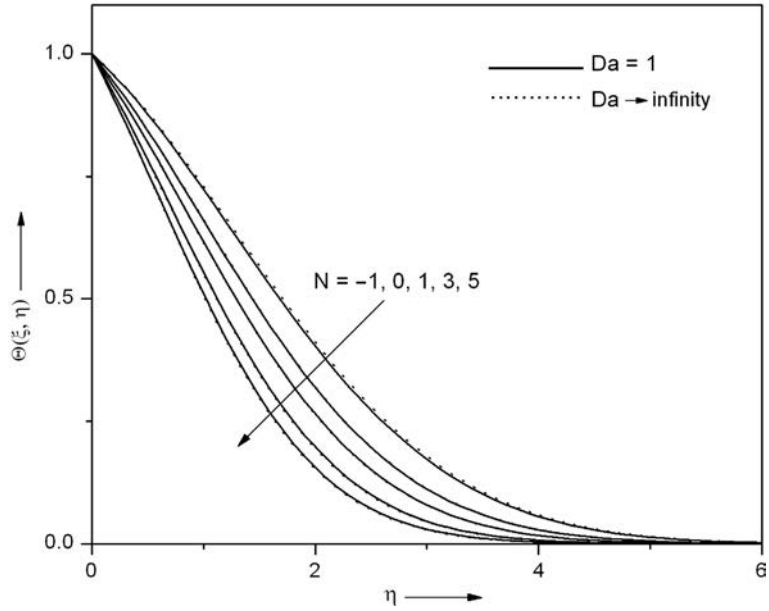
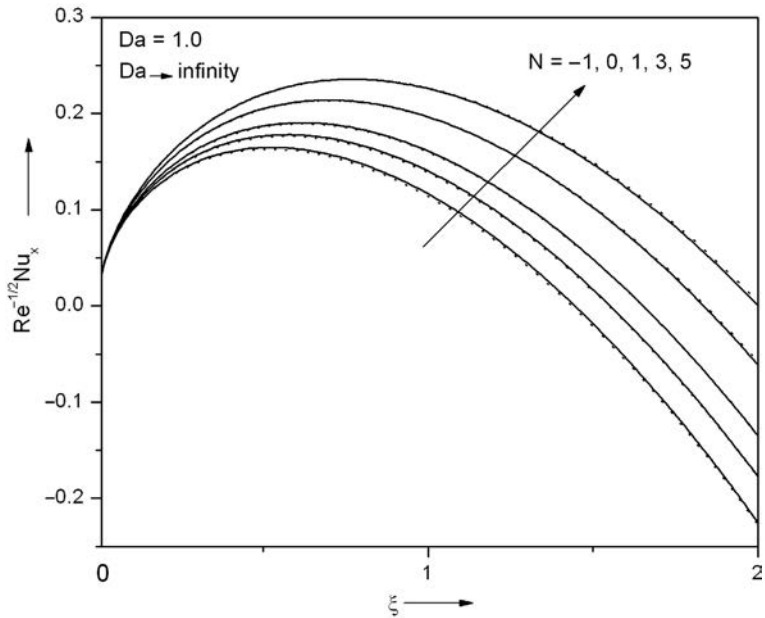


Figure 7.
Effects of N and Da on
heat transfer coefficient
for $Re = 10, \alpha = 0.5,$
 $\beta = 2, \lambda = 1, \Delta = 0.5,$
 $Q = 0.5, Pr = 0.7,$
 $Sc = 2.57$ and $\Gamma = 1$



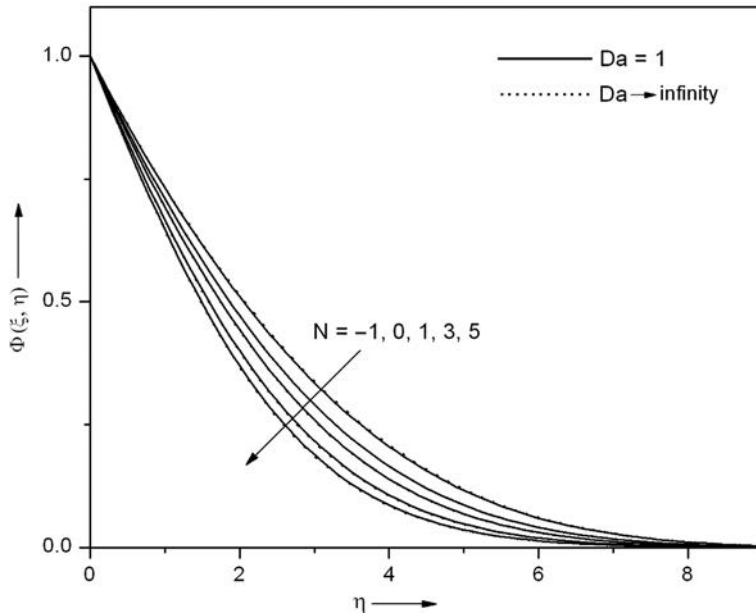


Figure 8.
Effects of N and Da on concentration profile for $\lambda = 2, \alpha = 1, \beta = 2, \Delta = 0.5, \xi = 0.5, \Gamma = 1, Re = 5, Sc = 0.22, Q = 0.5$ and $Pr = 0.7$

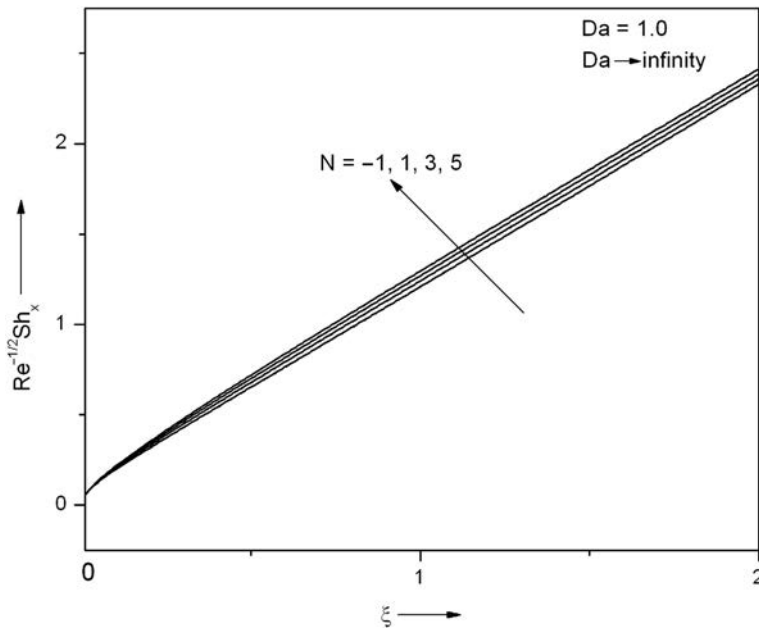


Figure 9.
Effects of N and Da on mass transfer coefficient for $Re = 10, \alpha = 0.5, \beta = 2, \lambda = 1, \Delta = 0.5, Q = 0.5, Pr = 0.7, Sc = 2.57$ and $\Gamma = 1$

the skin-friction coefficient increases. In particular for $Da = 1.0$ (porous medium present) at $\xi = 1.0$, the skin-friction coefficient ($Re^{1/2}C_f$) increases approximately 54 percent as N increases from 1.0 to 5.0 while for without the porous medium ($Da \rightarrow \infty$), the skin-friction coefficient ($Re^{1/2}C_f$) increases approximately 55 percent when N increases from $N = 1.0$ to 5.0.

In Figures 4 and 5, the angular velocity $\Omega(\xi, \eta)$ and the wall couple stress coefficient (C_{mf}) profiles are displayed for different values buoyancy ratio parameter (N) and Darcy number (Da), respectively. The negative values of the dimensionless angular velocity indicate that the micro-rotation of substructures in the polar fluid is clock-wise. It is observed that the variation of N leads to a decrease in the angular velocity. Further, the angular velocity is found to increase in the porous medium ($Da = 1.0$) for ($N < 0$), as compared to the case without a porous medium ($Da \rightarrow \infty$). The wall couple stress coefficient (C_{mf}) increases with N monotonously with increasing values of ξ . In particular, at $\xi = 1.0$, (C_{mf}) increases approximately 125 percent as N increases from 1.0 to 5.0 with a porous medium ($Da = 1.0$) while for the case without a porous medium ($Da \rightarrow \infty$), the wall couple stress coefficient (C_{mf}) increases approximately 131 percent when N increases from $N = 1.0$ to 5.0.

The temperature $\Theta(\xi, \eta)$ and heat transfer coefficient ($Re^{-1/2}Nu_x$) profiles are plotted in Figures 6 and 7 for different values buoyancy ratio parameter (N) and Darcy number (Da), respectively. The results indicate that an increase in the buoyancy ratio parameter (N) clearly induces a strong reduction in the temperature of the fluid and thus results into the thinner thermal boundary layer. It is further observed that the heat transfer coefficient ($Re^{-1/2}Nu_x$) increases with N near the surface and reduces further as it moves away from the surface. It is also observed that with $N \leq 0$, the heat transfer coefficient ($Re^{-1/2}Nu_x$) is found to reduce in the absence of the porous medium ($Da \rightarrow \infty$) near the surface as compared to the case when the porous medium is present ($Da = 1.0$). When $N > 0$, the heat transfer coefficient ($Re^{-1/2}Nu_x$) is found to increase away from the surface in the case when the porous medium is present as compared to the case without the porous medium ($Da \rightarrow \infty$). In particular, at $\xi = 1.0$, ($Re^{-1/2}Nu_x$) increases approximately 40 percent as N increases from 1.0 to 5.0 with the porous medium ($Da = 1.0$) while for the case without the porous medium ($Da \rightarrow \infty$), ($Re^{-1/2}Nu_x$) increases approximately 42 percent when N increases from $N = 1.0$ to 5.0.

In Figures 8 and 9, the concentration $\Phi(\xi, \eta)$ and the mass transfer coefficient ($Re^{-1/2}Sh_x$) profiles are depicted for different values of the buoyancy ratio parameter (N) and the Darcy number (Da), respectively. It is seen that the concentration profile decreases with increasing values of N . The concentration profiles remain unchanged with or without the porous medium. The behavior of the mass transfer rate ($Re^{-1/2}Sh_x$) is the same as in the case of the heat transfer coefficient ($Re^{-1/2}Nu_x$). In particular, at $\xi = 1.0$, ($Re^{-1/2}Sh_x$) increases approximately 5 percent as N increases from 1.0 to 5.0 in the presence of the porous medium ($Da = 1.0$) as well as in the absence of the porous medium ($Da \rightarrow \infty$).

The effects of the buoyancy parameter (λ) and material parameter (α) on the velocity $F(\xi, \eta)$, angular velocity $\Omega(\xi, \eta)$, temperature $\Theta(\xi, \eta)$ and concentration $\Phi(\xi, \eta)$ profiles are shown in Figures 10-17, respectively. The velocity $F(\xi, \eta)$ and the skin-friction coefficient ($Re^{1/2}C_f$) profiles are shown in Figures 10 and 11, respectively, for different values of buoyancy parameter (λ) and material parameter (α). It is observed from the Figure 6 that, for buoyancy aiding flow ($\lambda > 0$), the buoyancy force

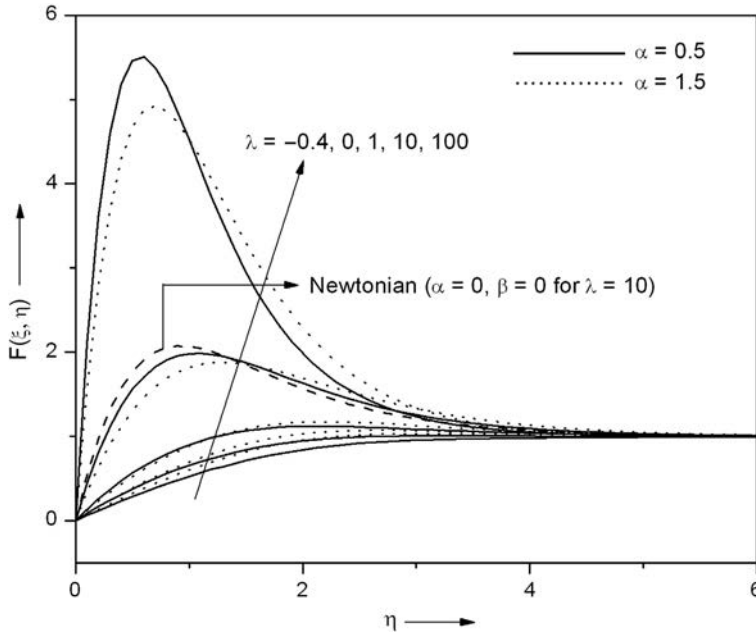


Figure 10. Effects of λ and α on velocity profile for $N = 1$, $Da = 1$, $\beta = 2$, $\Delta = 0.5$, $\xi = 0.5$, $\Gamma = 1$, $Re = 5$, $Sc = 0.22$, $Q = 0.5$ and $Pr = 0.7$

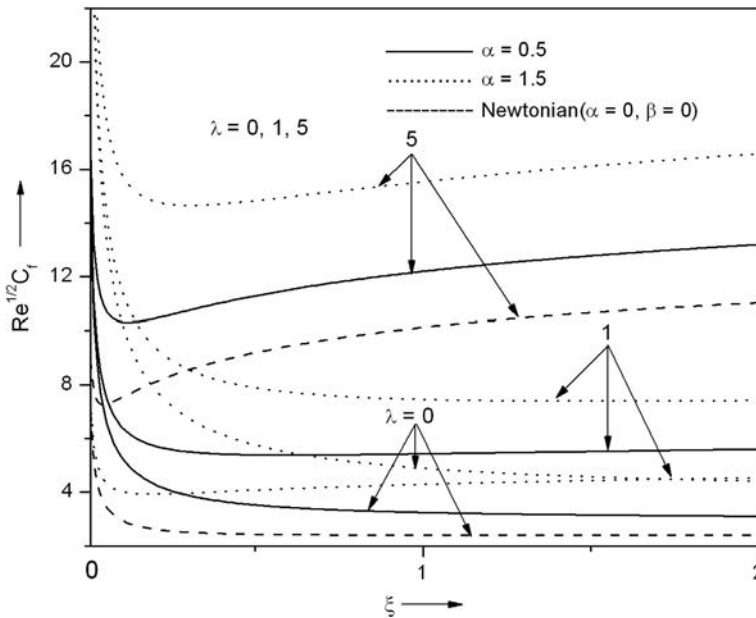


Figure 11. Effects of λ and α on skin-friction coefficient for $Re = 10$, $Da = 1$, $\beta = 2$, $N = 1$, $\Delta = 0.5$, $Q = 0.5$, $Pr = 0.7$, $Sc = 2.57$ and $\Gamma = 1$

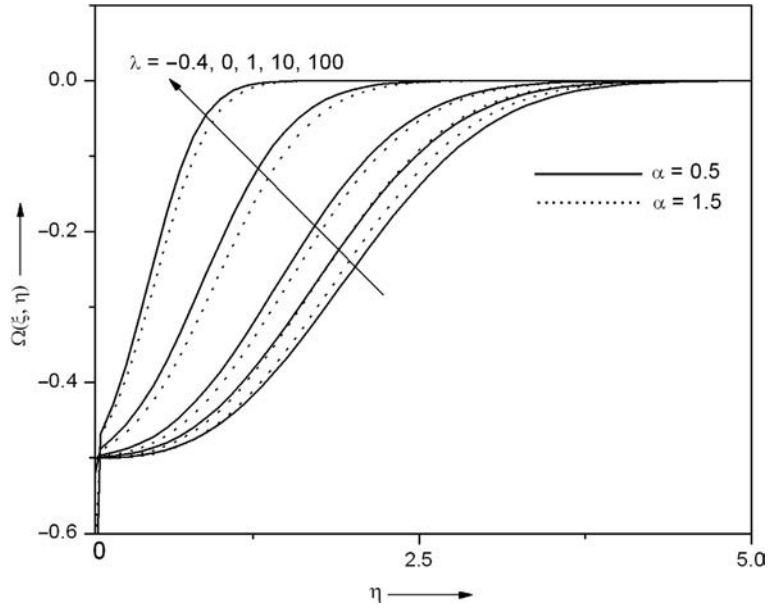


Figure 12.
Effects of λ and α on angular velocity profile for $N = 1$, $Da = 1$, $\beta = 2$, $\Delta = 0.5$, $\xi = 0.5$, $\Gamma = 1$, $Re = 5$, $Sc = 0.22$, $Q = 0.5$ and $Pr = 0.7$

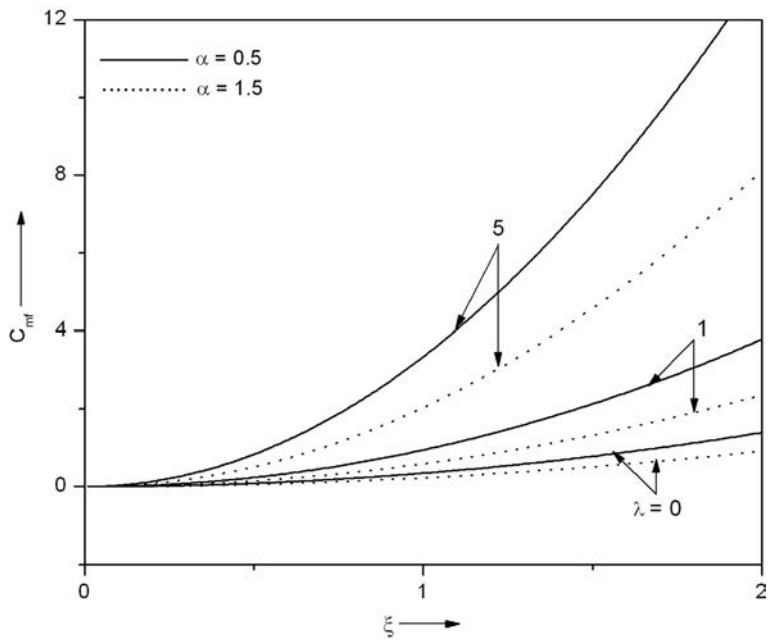


Figure 13.
Effects of λ and α on couple stress coefficient for $Re = 10$, $Da = 1$, $\beta = 2$, $N = 1$, $\Delta = 0.5$, $Q = 0.5$, $Pr = 0.7$, $Sc = 2.57$ and $\Gamma = 1$

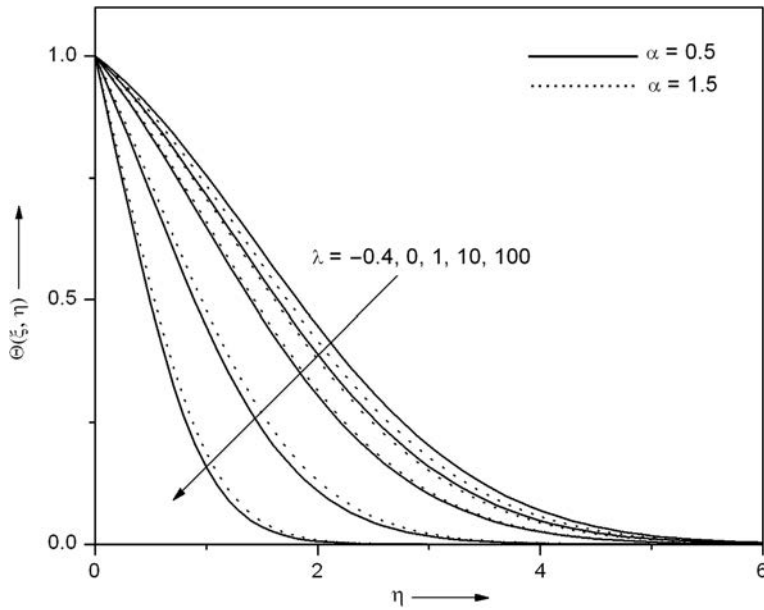


Figure 14. Effects of λ and α on temperature profile for $N = 1$, $Da = 1$, $\beta = 2$, $\Delta = 0.5$, $\xi = 0.5$, $\Gamma = 1$, $Re = 5$, $Sc = 0.22$, $Q = 0.5$ and $Pr = 0.7$

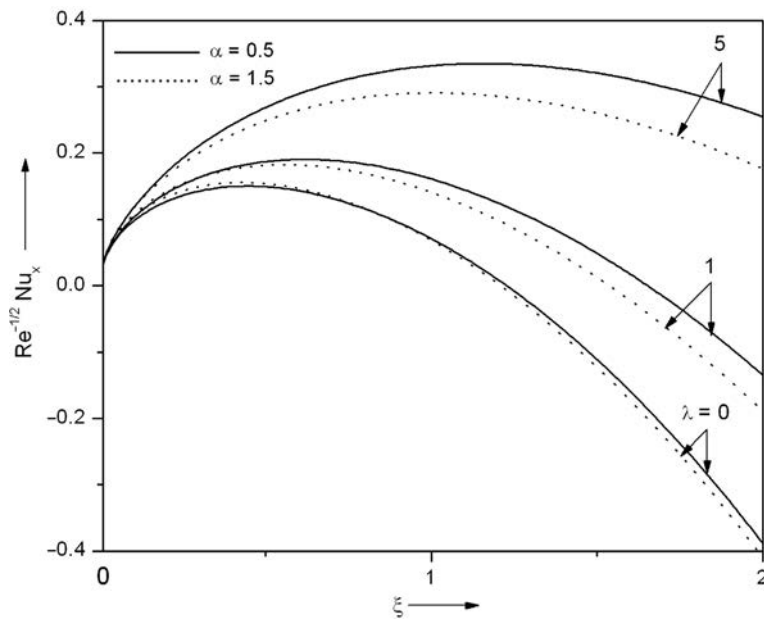


Figure 15. Effects of λ and α on heat transfer coefficient for $Re = 10$, $Da = 1$, $\beta = 2$, $N = 1$, $\Delta = 0.5$, $Q = 0.5$, $Pr = 0.7$, $Sc = 2.57$ and $\Gamma = 1$

Figure 16.
Effects of λ and α on concentration profile for $N = 1$, $Da = 1$, $\beta = 2$, $\Delta = 0.5$, $\xi = 0.5$, $\Gamma = 1$, $Re = 5$, $Sc = 0.22$, $Q = 0.5$ and $Pr = 0.7$

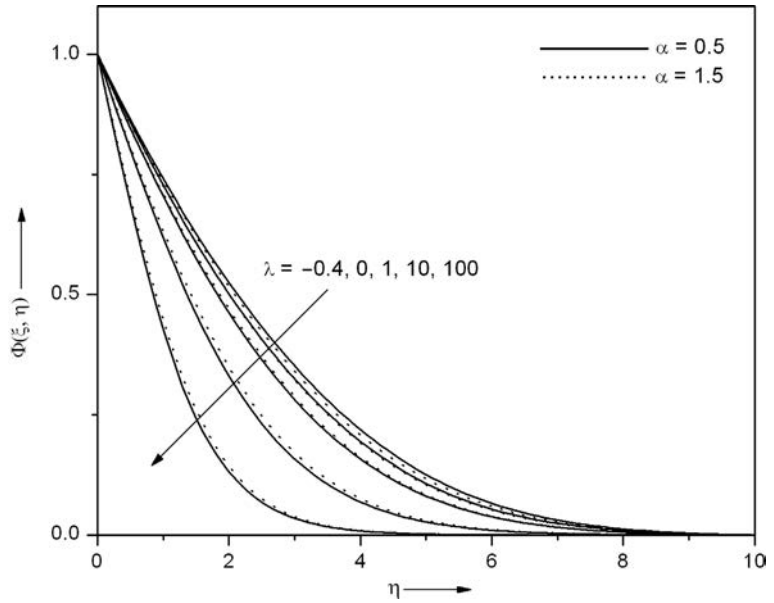
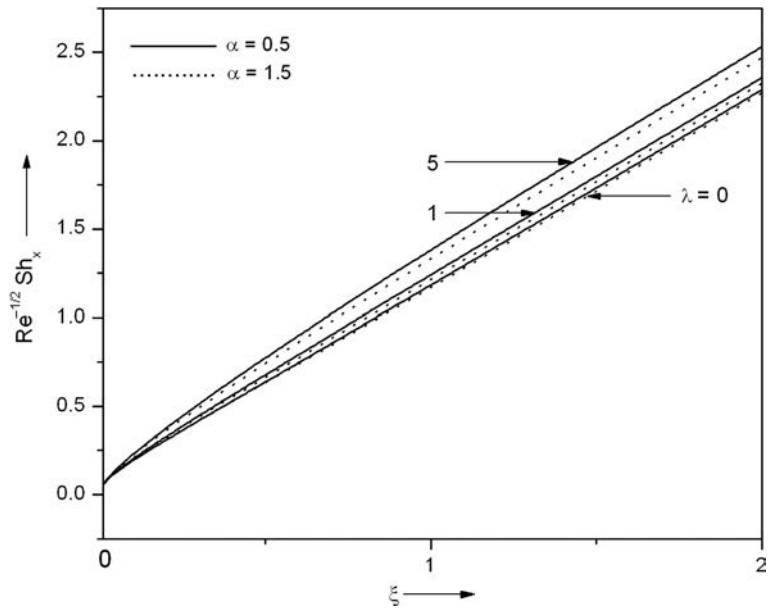


Figure 17.
Effects of λ and α on mass transfer coefficient for $Re = 10$, $Da = 1$, $\beta = 2$, $N = 1$, $\Delta = 0.5$, $Q = 0.5$, $Pr = 0.7$, $Sc = 2.57$ and $\Gamma = 1$



shows significant overshoot in the velocity profiles with the material parameter α . As explained before, the physical reason is that the due to combined effects of assisting buoyancy forces due to thermal and concentration gradients and heat generation acts like a favorable pressure gradient which enhances the fluid acceleration. Further, it is observed that the velocity decreases with increasing values of the material parameter α near the surface and further, increases as it moves away from the surface. However, the velocity of the polar fluid flow decreases as compared to the Newtonian fluid case ($\alpha = 0, \beta = 0$). The effects of the buoyancy parameter (λ) and material parameter (α) on the skin-friction coefficient ($Re^{1/2}C_f$) when $N = 1.0, \beta = 2.0, Sc = 2.57, \Delta = 0.5, Pr = 0.7, Re = 10.0, Da = 1.0, \Gamma = 1$ and $Q = 0.5$ are shown in Figure 11. It is observed that the skin-friction coefficient ($Re^{1/2}C_f$) increases with the buoyancy parameter (λ) considerably. This is due to the fact that the increase of (λ) enhances the fluid acceleration and hence, the skin-friction coefficient ($Re^{1/2}C_f$) increases. In particular, for $\alpha = 0.5$ at $\xi = 1.0$, the skin-friction coefficient ($Re^{1/2}C_f$) increases approximately 125 percent as λ increases from 1.0 to 5.0 while for $\alpha = 1.5$ the skin-friction coefficient ($Re^{1/2}C_f$) increases approximately 108 percent when λ increases from $\lambda = 1.0$ to 5.0. However, the skin-friction coefficient ($Re^{1/2}C_f$) for the Newtonian fluid case ($\alpha = 0, \beta = 0$) increases approximately 136 percent when λ increases from $\lambda = 1.0$ to 5.0. The angular velocity $\Omega(\xi, \eta)$ and wall couple stress coefficient (C_{mf}) profiles are plotted in Figures 12 and 13, respectively, for different values buoyancy parameter (λ) and material parameter (α). It is noted that the variation of λ leads to a considerable decrease (in magnitude) in the angular velocity. Further, the angular velocity is found to decrease with an increasing value of the material parameter (α). The wall couple stress coefficient (C_{mf}) increases with λ monotonously for increasing values of ξ . In particular, at $\xi = 1.0$, (C_{mf}) increases approximately 252 percent as λ decreases from 1.0 to 5.0 when $\alpha = 0.5$ while for $\alpha = 1.5$ the wall couple stress coefficient (C_{mf}) increases approximately 244 percent when λ decreases from $\lambda = 1.0$ to 5.0.

The effects of the buoyancy forces parameter (λ) and the material parameter (α) on temperature $\Theta(\xi, \eta)$ and heat transfer rate ($Re^{-1/2}Nu_x$) profiles are shown in Figures 14 and 15. These results indicate that an increase in the material parameter (α) clearly induces a strong increase in the temperature of the fluid and thus, resulting in a thicker thermal boundary layer while an increase in the buoyancy parameter (λ) induces a strong reduction in the fluid temperature and hence, yielding a thinner thermal boundary layer. It is further observed that the heat transfer coefficient ($Re^{-1/2}Nu_x$) increases with (λ) near the plate and decreases steadily with increasing values of ξ while it decreases with increasing values of the material parameter (α) throughout. In particular, at $\xi = 1.0$, ($Re^{-1/2}Nu_x$) decreases approximately 106 percent as (λ) increases from 1.0 to 5.0 for both at $\alpha = 0.5$ as well as $\alpha = 1.5$.

Figures 16 and 17 show the influence of the buoyancy parameter (λ) and the material parameter (α) on the concentration $\Phi(\xi, \eta)$ and mass transfer rate ($Re^{-1/2}Sh_x$), respectively. It is noted that an increase in the value of (λ) leads to a fall in the concentration profile while it enhances as the material parameter (α) increases. It is further observed that the mass transfer coefficient ($Re^{-1/2}Sh_x$) increases monotonously with (λ) for increasing values of ξ while it decreases with increasing values of the material parameter (α). In particular, at $\xi = 1.0$, ($Re^{-1/2}Sh_x$) increases approximately 11 percent as (λ) increases from 1.0 to 5.0 for $\alpha = 0.5$ while for $\alpha = 1.5$, ($Re^{-1/2}Sh_x$) increases approximately 10 percent when (λ) increases from 1.0 to 5.0.

The effects of the material parameters (α) and (β) on the velocity $F(\xi, \eta)$ and the angular velocity $\Omega(\xi, \eta)$ profiles are shown in Figures 18-21. Figures 18 and 19 show the velocity $F(\xi, \eta)$ and the skin-friction coefficient ($Re^{1/2}C_f$) profiles for different values of the material parameter β , respectively. It is noted that the velocity profile decreases with increasing values of the material parameters (α) and (β). It clearly indicates that couple stresses are dominant during the rotation of the particles. It is further noted that the skin-friction coefficient ($Re^{1/2}C_f$) increases slightly with increasing values of the material parameters (α) and (β). In particular, at $\xi = 1.0$, ($Re^{1/2}C_f$) increases approximately 2 percent as (β) increases from 2.0 to 10.0 for $\alpha = 0.5$ while for $\alpha = 1.5$, ($Re^{1/2}C_f$) increases approximately 4 percent when (β) increases from 2.0 to 10.0.

Figures 20 and 21 show the angular velocity $\Omega(\eta)$ and the wall couple stress coefficient (C_{mf}) profiles for different values of the material parameter β , respectively. It is observed that the effects of the material parameter β on the dimensionless angular velocity are significant. An increase in the value of the material parameter β causes a rise in the dimensionless angular velocity which clearly indicates that the couple stresses are dominant during the rotation of the particles. The effects of (α) and (β) (the material parameters) on the wall couple stress coefficient (C_{mf}) when $\lambda = 5.0$, $Da = 1.0$, $N = 1.0$, $Sc = 2.57$, $\Delta = 0.5$, $Pr = 0.7$, $Re = 10.0$, $\Gamma = 1$ and $Q = 0.5$ are shown in Figure 21. It is observed that the wall couple stress coefficient (C_{fm}) increases as β increases significantly with increasing values of ξ . In particular, at $\xi = 1.0$, (C_{mf}) decreases approximately 80 percent as (β) increases from 2.0 to 10.0 for both cases at $\alpha = 0.5$ as well as at $\alpha = 1.5$.

The effects of the heat generation or absorption parameter (Q) and the Prandtl number (Pr) on the temperature $\Theta(\xi, \eta)$ profile are shown in Figure 22 for $\lambda = 2.0$, $Sc = 0.22$, $N = 1.0$, $\Delta = 0.5$, $Re = 10.0$, $\xi = 1.0$, $Da = 1.0$, $\beta = 2.0$, $\Gamma = 1$ and $\alpha = 1.0$.

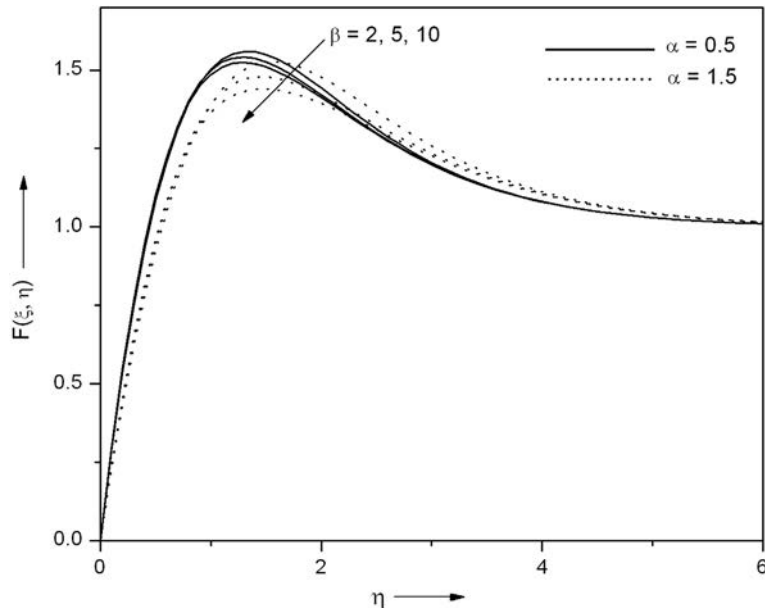


Figure 18.
Effects of β and α on velocity profile for $N = 1$, $Da = 1$, $\lambda = 5$, $\Delta = 0.5$, $\xi = 0.5$, $\Gamma = 1$, $Re = 5$, $Sc = 0.22$, $Q = 0.5$ and $Pr = 0.7$

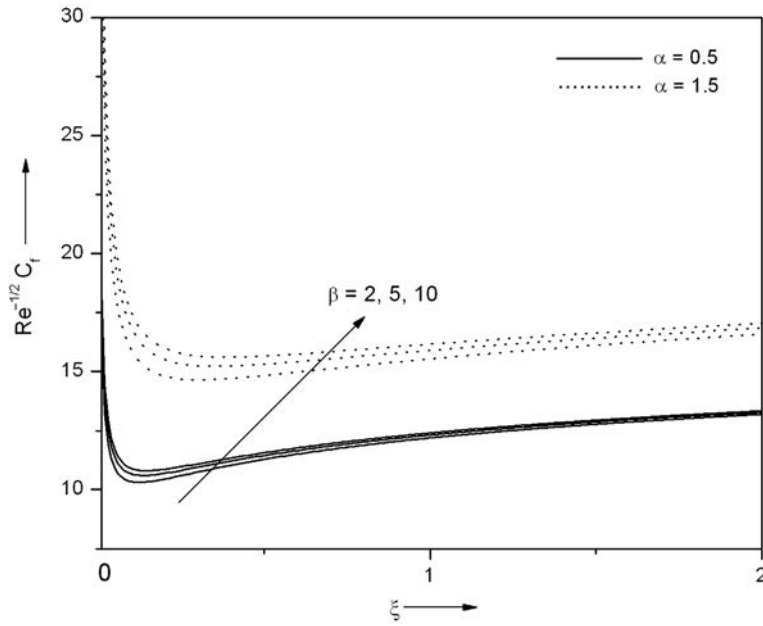


Figure 19.
Effects of α and β on skin-friction coefficient for $Re = 10$, $Da = 1$, $\lambda = 5$, $N = 1$, $\Delta = 0.5$, $Q = 0.5$, $Pr = 0.7$, $Sc = 2.57$ and $\Gamma = 1$

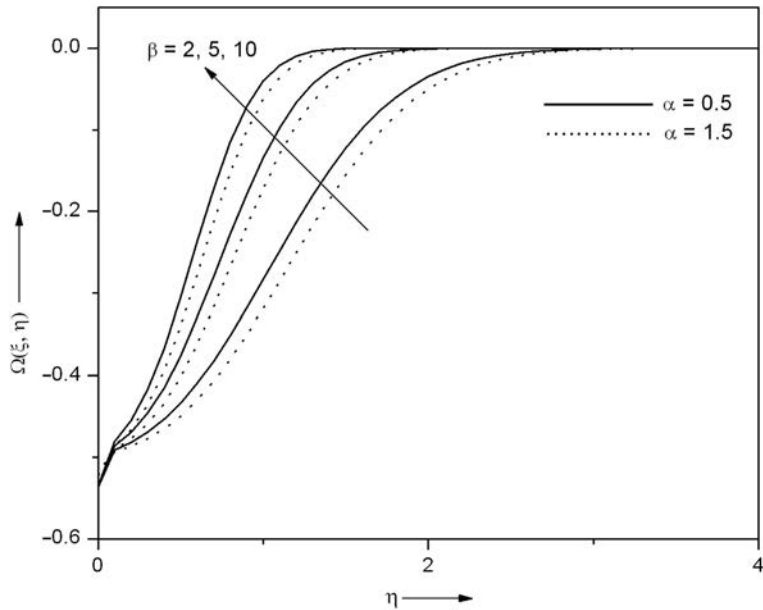


Figure 20.
Effects of β and α on angular velocity profile for $N = 1$, $Da = 1$, $\lambda = 5$, $\Delta = 0.5$, $\xi = 0.5$, $\Gamma = 1$, $Re = 5$, $Sc = 0.22$, $Q = 0.5$ and $Pr = 0.7$

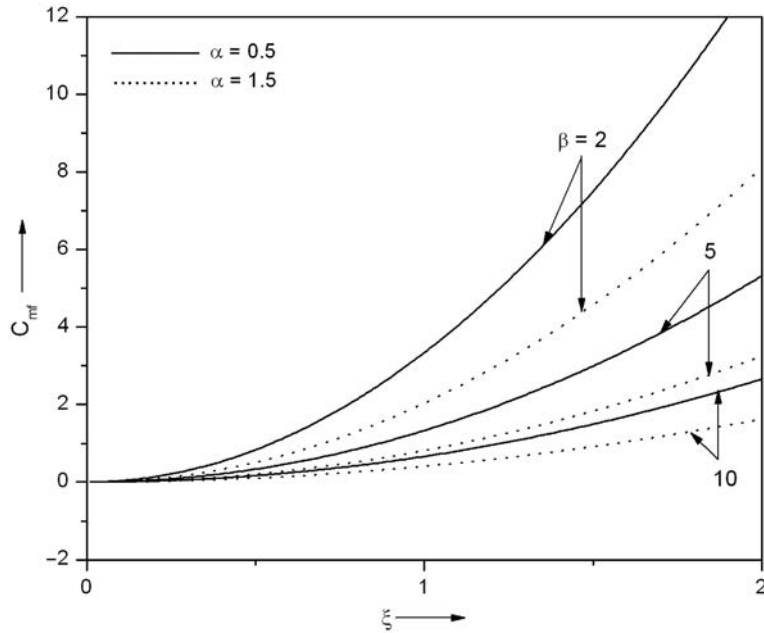


Figure 21.
Effects of α and β on skin-friction coefficient for $Re = 10$, $Da = 1$, $\lambda = 5$, $N = 1$, $\Delta = 0.5$, $Q = 0.5$, $Pr = 0.7$, $Sc = 2.57$ and $\Gamma = 1$

It is noted that owing to the presence of heat generation or a heat source effect ($Q > 0$) within the boundary layer, the thermal state of the fluid increases. As a result, the temperature of the fluid increases everywhere away from the boundaries for which it is maintained constant there. Further, the thermal boundary layer thickness and the negative wall slope of the temperature distribution enhance. Conversely, the presence of heat absorption or a heat sink effect ($Q < 0$) within the boundary layer produces the opposite effect, namely, it has the tendency to reduce the fluid temperature, the thermal boundary layer thickness and the negative wall slope of the temperature distribution. This causes the thermal buoyancy effects to decrease resulting in a net reduction in the fluid velocity. These behaviors are clearly observed from Figure 22 in which the magnitude of temperature field decreases for ($Q < 0$). Moreover, it is also observed that the thickness of the thermal (temperature) boundary layer decreases as the heat absorption or heat sink effect increases. Figure 23 shows the variations of the heat transfer coefficient ($Re^{-1/2}Nu_x$) for different values of the heat generation or absorption parameter (Q), for $\lambda = 2.0$, $Sc = 2.57$, $N = 1.0$, $\Delta = 0.5$, $Re = 10.0$, $\xi = 1.0$, $Da = 1.0$, $\beta = 2.0$, $\Gamma = 1$ and $\alpha = 1.0$, respectively. It is clear from the Figure 23 that increasing the heat generation parameter Q results in increases in the skin-friction coefficient and decreases in the heat transfer rate ($Re^{-1/2}Nu_x$). In addition, it is seen that the effect of increasing the Prandtl number Pr is to enhance the heat transfer rate and to decrease the skin-friction coefficient due to reduction in the fluid velocity. It should be noted that as the Prandtl number Pr increases, both the fluid temperature and velocity decrease. As a result, the negative wall slopes of the temperature distribution increases generating an increase in the local Nusselt number and a decrease in the skin-friction coefficient. The opposite effect is obtained for heat absorption effects. In particular, at $\xi = 1.0$, ($Re^{-1/2}Nu_x$) increases approximately 22 percent as (Q) increases from 0.0 to 1.0

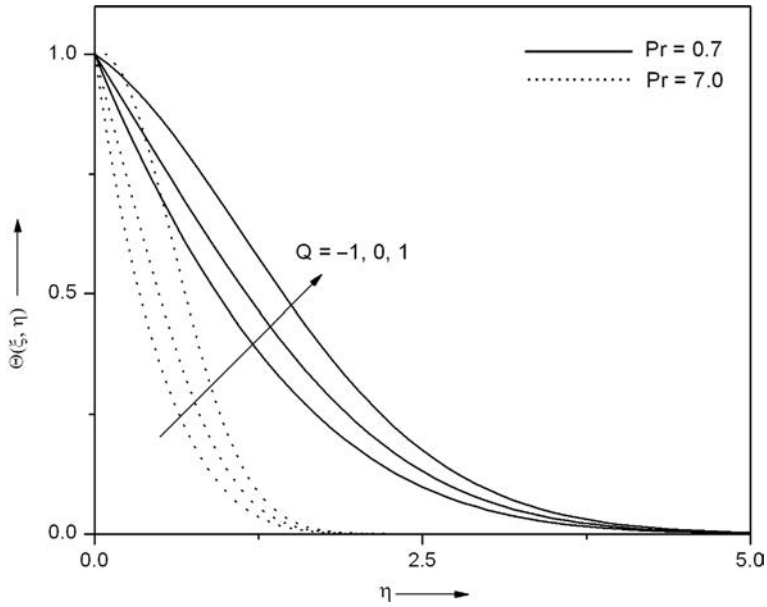


Figure 22. Effects of Q and Pr on temperature profile for $N = 1$, $Da = 1$, $\lambda = 2$, $\Delta = 0.5$, $\xi = 0.5$, $\Gamma = 1$, $Re = 5$, $Sc = 0.22$, $\alpha = 1$ and $\beta = 2$

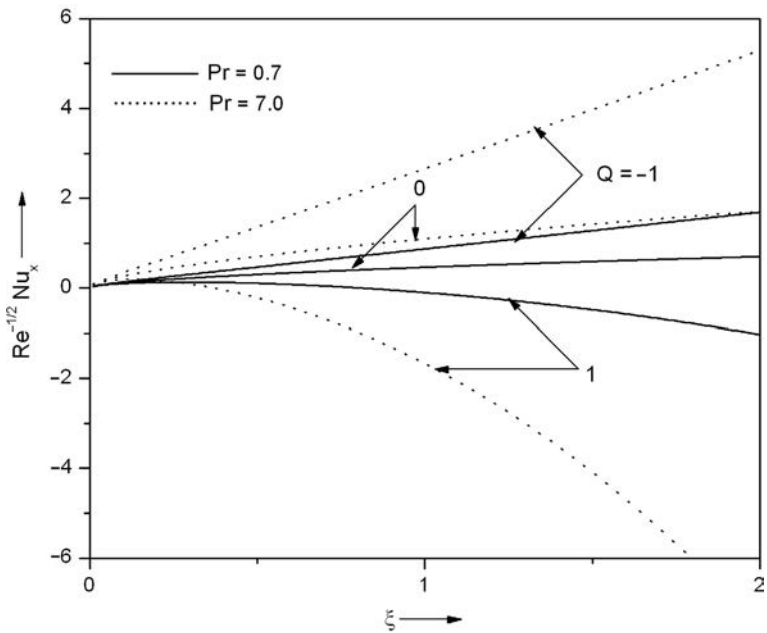


Figure 23. Effects of Q and Pr on heat transfer rate for $Re = 10$, $Da = 1$, $\lambda = 2$, $N = 1$, $\Delta = 0.5$, $\alpha = 1$, $\beta = 2$, $Sc = 2.57$ and $\Gamma = 1$

for $Pr = 0.7$ while for $Pr = 7.0$, $(Re^{-1/2}Nu_x)$ increases approximately 253 percent when (Q) increases from 0.0 to 1.0.

Figures 24 and 25 shows the variations of the concentration $\Phi(\xi, \eta)$ and the mass transfer rate $(Re^{-1/2}Sh_x)$ profiles for various values of the Schmidt number Sc and the chemical reaction parameter Δ , respectively. It shows that the magnitude of the velocity and concentration distributions increase when the chemical reaction parameter $\Delta < 0$ (species consumption or destructive chemical reaction) is increased. An increase in the concentration of the diffusing species increases the mass diffusion and, in turn, the fluid velocity and temperature increase. On the contrary, for $\Delta > 0$ (species generation or constructive chemical reaction) as Δ increases, the velocity distribution decreases so that the concentration reduces. The values of the Schmidt number (Sc) are chosen to be more realistic, 0.22 and 2.57, representing diffusing chemical species of most common interest like water and Propyl Benzene, etc. at 25°C at one atmospheric pressure. It is observed that the concentration and velocity boundary layers are decreased as the Schmidt number Sc is increased. The physical reason is that the Schmidt number Sc leads to a thinning of the concentration boundary layer. As a result, the concentration of the fluid decreases and this leads to a decrease in the fluid velocity. The variation of the mass transfer rate $(Re^{-1/2}Sh_x)$ is shown in Figure 25. The mass transfer rate $(Re^{-1/2}Sh_x)$ increases for $\Delta > 0$ while it decreases for $\Delta < 0$. In particular, at $\xi = 1.0$, $(Re^{-1/2}Sh_x)$ increases approximately 34 percent as (Δ) increases from 0.0 to 1.0 for $Sc = 0.22$ while for $Sc = 2.57$, $(Re^{-1/2}Sh_x)$ increases approximately 56 percent when (Δ) increases from 0.0 to 1.0. However, the mass transfer coefficient $(Re^{-1/2}Sh_x)$ decreases approximately 93 percent as (Δ) decreases from 0.0 to -1.0 for $Sc = 0.22$ while for $Sc = 2.57$, $(Re^{-1/2}Sh_x)$ decreases approximately about 154 percent when (Δ) decreases from 0.0 to -1.0 .

Figures 26 and 27 shows the variations of the velocity profile $F(\xi, \eta)$ and the skin-friction coefficient $(Re^{1/2}C_f)$ for various values of the Forchheimer's drag

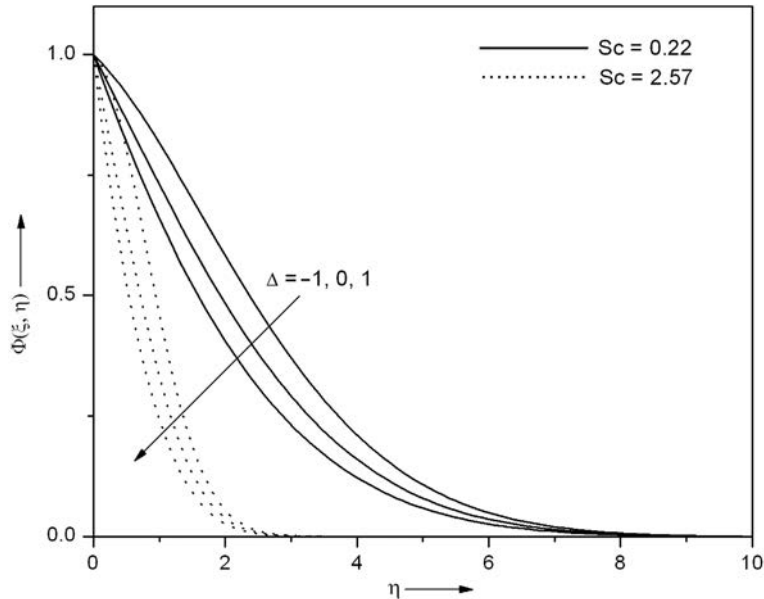


Figure 24.
Effects of Δ and Sc on
concentration profile for
 $N = 1, Da = 1, \lambda = 2,$
 $Q = 0.5, \xi = 0.5, \Gamma = 1,$
 $Re = 5, Pr = 0.7, \alpha = 1$
and $\beta = 2$

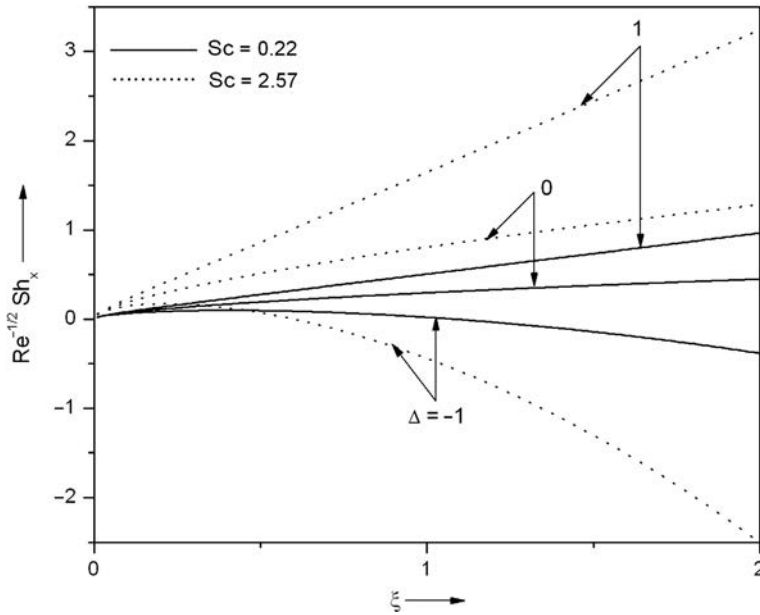


Figure 25.
Effects of Δ and Sc on heat transfer rate for $Re = 10$, $Da = 1$, $\lambda = 2$, $N = 1$, $Q = 0.5$, $\alpha = 1$, $\beta = 2$, $Pr = 0.7$ and $\Gamma = 1$

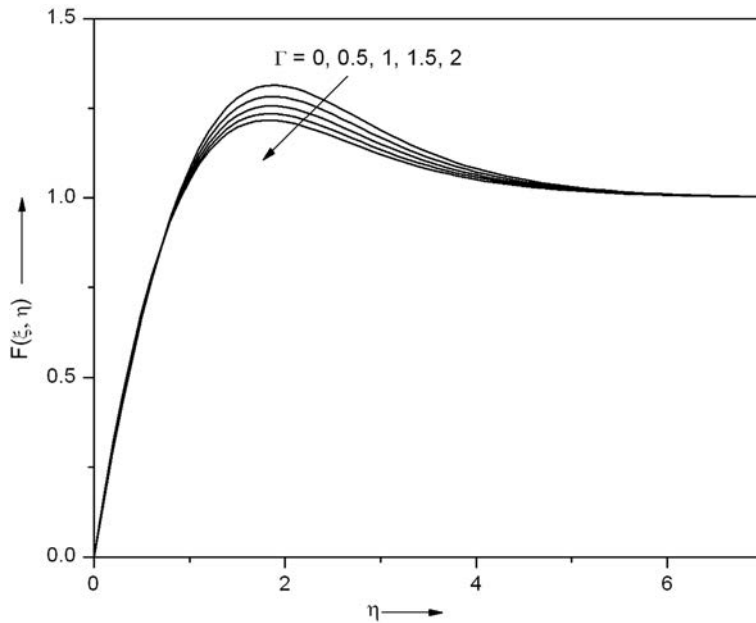


Figure 26.
Effects of Γ on velocity profile for $N = 1$, $Da = 1$, $\beta = 2$, $\lambda = 2$, $\Delta = 1$, $\xi = 0.5$, $\alpha = 1$, $Re = 5$, $Sc = 0.22$, $Q = 1$ and $Pr = 0.7$

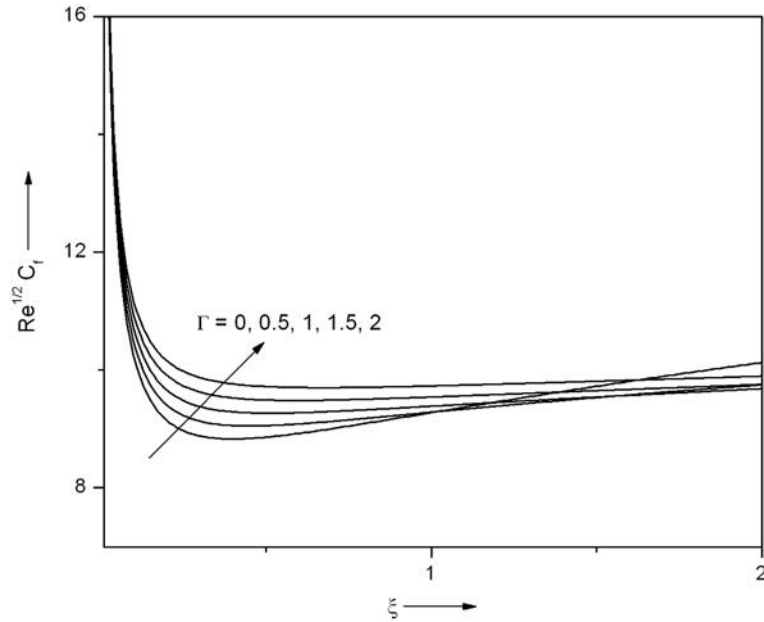


Figure 27.
Effects of Γ on skin-friction coefficient for $Re = 10$, $Da = 1$, $\lambda = 2$, $N = 1$, $\Delta = 1$, $\alpha = 1$, $\beta = 2$, $Sc = 0.22$, $Q = 0.5$ and $Pr = 0.7$

parameter Γ when $\lambda = 2.0$, $Sc = 2.57$, $N = 1.0$, $\Delta = 0.5$, $Re = 10.0$, $\xi = 1.0$, $Da = 1.0$, $\beta = 2.0$ and $\alpha = 1.0$, respectively. It shows that the magnitude of the velocity distribution decreases when Forchheimer's drag parameter Γ is increased while the skin-friction coefficient ($Re^{1/2}C_f$) increases for an increasing value of Forchheimer's drag parameter Γ . In particular, ($Re^{1/2}C_f$) increases approximately about 5 percent when Γ increases from 0.0 to 2.0 at $\xi = 1$.

5. Conclusions

A detailed numerical study was carried out for mixed convection flow of a polar fluid along a vertical plate embedded in a non-Darcian porous medium in the presence of internal heat generation or absorption and a homogeneous first-order chemical reaction. The governing equations are formulated and transformed into a set of non-similar differential equations using suitable variable transformations. This set of non-similar, coupled, nonlinear, partial differential equations is solved using an implicit finite-difference scheme in combination with quasi-linearization technique. Conclusions of the study are as follows:

- The buoyancy parameter λ and the ratio of buoyancy forces N cause overshoot in the velocity profile.
- The effects of the material parameters α and β on the velocity, angular velocity, temperature and the concentration profile are significant.
- The velocity of the polar fluid is lower as compared to the Newtonian fluid velocity under the same conditions.
- Higher Prandtl numbers $Pr = 7.0$ (water) cause thinner thermal boundary layers in the presence of heat generation or absorption ($Q > 0$ or $Q < 0$). The heat

generation effect ($Q > 0$) causes thicker velocity and thermal boundary layers while the heat absorption effect ($Q < 0$) has the tendency to reduce the velocity and thermal boundary-layer thicknesses.

- The velocity profile decreases in the presence of a porous medium as compared to the case without a porous medium.
- The velocity profile decreases as Forchheimer's drag parameter Γ increases.
- The effects of the chemical reaction parameter Δ and the Schmidt number Sc are significant on the concentration and mass transfer rate.

References

- Aero, E.L., Bulygin, A.N. and Kuvshinski, E.V. (1965), "Asymmetric hydromechanics", *Prikl. Math. Mech.*, Vol. 29 No. 2, pp. 297-308 (*J. Appl. Math. Mech.*, Vol. 29, pp. 333-346).
- Aly, E.H., Elliot, L. and Ingham, D.B. (2003), "Mixed convection boundary layer flow over a vertical surface embedded in a porous medium", *European Journal of Mechanics: B, Fluids*, Vol. 22, pp. 529-543.
- Bejan, A., Dincer, I., Lorente, S., Miguel, A.F. and Reis, A.H. (2004), *Porous and Complex Flow Structures in Modern Technologies*, Springer, New York, NY.
- Chin, K.E., Nazar, R., Arifin, N.M. and Pop, I. (2007), "Effect of variable viscosity on mixed convection boundary layer flow over a vertical surface embedded in a porous medium", *International Communications in Heat Mass Transfer*, Vol. 34, pp. 464-473.
- Cowin, S.C. (1974), "The theory of polar fluids", *Advances in Applied Mechanics*, Vol. 14, pp. 279-347.
- D'ep, N.V. (1968), "Equations of a fluid boundary layer with couple stresses", *Prikl. Math. Mech.*, Vol. 32, pp. 748-753 (*J. Appl. Math. Mech.*, Vol. 32, pp. 777-783 (1968)).
- Helmy, K.A. (1998), "MHD unsteady free convection flow past a vertical porous plate", *ZAMM*, Vol. 78, pp. 255-270.
- Hiremath, P.S. and Patil, P.M. (1993), "Free convection effects on the oscillatory flow of a couple stress fluid through a porous medium", *Acta Mechanica*, Vol. 98, pp. 143-158.
- Hossain, M.A., Banu, N. and Nakayama, A. (1994), "Non-darcy forced convection boundary layer flow over a wedge embedded in a saturated porous medium", *Numerical Heat Transfer, Part A*, Vol. 26, pp. 399-414.
- Ingham, D.B. and Pop, I. (Eds) (2005), *Transport Phenomena in Porous Media*, Elsevier, Oxford.
- Ingham, D.B., Bejan, A., Mamut, E. and Pop, I. (Eds) (2004), *Emerging Technologies and Techniques in Porous Media*, Kluwer, Dordrecht.
- Inouye, K. and Tate, A. (1974), "Finite difference version quasilinearisation applied to boundary layer equations", *AIAA Journal*, Vol. 12, pp. 558-560.
- Kandasamy, R., Perisamy, K. and Sivagnana Prabhu, K.K. (2005a), "Chemical reaction, heat and mass transfer on MHD flow over a vertical stretching surface with heat source and thermal stratification effects", *International Journal of Heat Mass Transfer*, Vol. 48, pp. 4557-4561.
- Kandasamy, R., Perisamy, K. and Sivagnana Prabhu, K.K. (2005b), "Effects of chemical reaction, heat and mass transfer along a wedge with heat source and concentration in the presence of suction or injection", *International Journal of Heat Mass Transfer*, Vol. 48, pp. 1388-1394.
- Kim, Y.J. (2001), "Unsteady MHD convection flow of polar fluids past a vertical moving porous plate in a porous medium", *International Journal of Heat Mass Transfer*, Vol. 44, pp. 2791-2799.

- Merkin, J.H. (1980), "Mixed convection boundary layer flow on a vertical surface in a saturated porous medium", *Journal of Engineering Mathematics*, Vol. 14, pp. 301-303.
- Merkin, J.H. (1985), "On dual solutions occurring in mixed convection in a porous medium", *Journal of Engineering Mathematics*, Vol. 20, pp. 171-179.
- Nazar, R. and Pop, I. (2004), "Mixed convection boundary layer flow over a vertical surface in a porous medium with variable surface heat flux", *Recent Advances and Applications in Heat and Mass Transfer IMECE, Kuwait*, pp. 87-97.
- Nield, D.A. and Bejan, A. (2006), *Convection in Porous Media*, 3rd ed., Springer, New York, NY.
- Ogulu, A. (2005), "On the oscillating plate temperature flow of a polar fluid past a vertical porous plate in the presence of couple stresses and radiation", *International Communications in Heat Mass Transfer*, Vol. 32, pp. 1231-1243.
- Patil, P.M. (2008), "Effects of free convection on the oscillatory flow of a polar fluid through a porous medium in the presence of variable heat flux", *Journal of Engineering Physics and Thermophysics*, Vol. 81 No. 5, pp. 905-922.
- Patil, P.M. and Hiremath, P.S. (1992), "A note on the effect of couple stresses on the flow through a porous medium", *Rheologica Acta*, Vol. 21, pp. 206-207.
- Patil, P.M. and Kulkarni, P.S. (2008), "Effects of chemical reaction on free convective flow of a polar fluid through a porous medium in the presence of internal heat generation", *International Journal of Thermal Sciences*, Vol. 47, pp. 1043-1054.
- Patil, P.M. and Kulkarni, P.S. (2009), "Free convective oscillatory flow of a polar fluid through a porous medium in the presence of oscillating suction and temperature", *Journal of Engineering Physics and Thermophysics*, Vol. 82 No. 6, pp. 1138-1145.
- Patil, P.M., Roy, S. and Chamkha, A.J. (2010), "Mixed convection flow over a vertical power law stretching sheet", *International Journal of Numerical Methods for Heat & Fluid Flow*, Vol. 20 No. 4, pp. 445-458.
- Raptis, A. and Perdikis, C. (2006), "Viscous flow over a non-linearly stretching sheet in the presence of a chemical reaction and magnetic field", *International Journal of Nonlinear Mechanics*, Vol. 42, pp. 527-529.
- Raptis, A. and Takhar, H.S. (1999), "Polar fluid through a porous medium", *Acta Mechanica*, Vol. 135, pp. 91-93.
- Schlichting, H. (2000), *Boundary Layer Theory*, Springer, New York, NY.
- Seddeek, M.A. (2005), "Finite element method for the effects of chemical reaction, variable viscosity, thermophoresis and heat generation/absorption on a boundary layer hydromagnetic flow with heat and mass transfer over a heat surface", *Acta Mechanica*, Vol. 177, pp. 1-18.
- Vafai, K. (Ed.) (2005), *Handbook of Porous Media*, 2nd ed., Taylor & Francis, New York, NY.
- Varga, R.S. (2000), *Matrix Iterative Analysis*, Prentice-Hall, Upper Saddle River, NJ.

Corresponding author

Ali J. Chamkha can be contacted at: achamkha@yahoo.com